Heidarzadeh *et al. Geosci. Lett. (2017) 4:31*
https://doi.org/10.1186/s40562-017-0097-0

Geoscience Letters

RESEARCH LETTER

Open Access

Bodrum–Kos (Turkey–Greece) Mw 6.6 earthquake and tsunami of 20 July 2017: a test for the Mediterranean tsunami warning system

Mohammad Heidarzadeh[1*], Ocal Necmioglu[2], Takeo Ishibe[3] and Ahmet C. Yalciner[4]

Abstract

Various Tsunami Service Providers (TSPs) within the Mediterranean Basin supply tsunami warnings including CAT-INGV (Italy), KOERI-RETMC (Turkey), and NOA/HL-NTWC (Greece). The 20 July 2017 Bodrum–Kos (Turkey–Greece) earthquake (Mw 6.6) and tsunami provided an opportunity to assess the response from these TSPs. Although the Bodrum–Kos tsunami was moderate (e.g., runup of 1.9 m) with little damage to properties, it was the first noticeable tsunami in the Mediterranean Basin since the 21 May 2003 western Mediterranean tsunami. Tsunami waveform analysis revealed that the trough-to-crest height was 34.1 cm at the near-field tide gauge station of Bodrum (Turkey). Tsunami period band was 2–30 min with peak periods at 7–13 min. We proposed a source fault model for this tsunami with the length and width of 25 and 15 km and uniform slip of 0.4 m. Tsunami simulations using both nodal planes produced almost same results in terms of agreement between tsunami observations and simulations. Different TSPs provided tsunami warnings at 10 min (CAT-INGV), 19 min (KOERI-RETMC), and 18 min (NOA/HL-NTWC) after the earthquake origin time. Apart from CAT-INGV, whose initial Mw estimation differed 0.2 units with respect to the final value, the response from the other two TSPs came relatively late compared to the desired warning time of ~ 10 min, given the difficulties for timely and accurate calculation of earthquake magnitude and tsunami impact assessment. It is argued that even if a warning time of ~ 10 min was achieved, it might not have been sufficient for addressing near-field tsunami hazards. Despite considerable progress and achievements made within the upstream components of NEAMTWS (North East Atlantic, Mediterranean and Connected seas Tsunami Warning System), the experience from this moderate tsunami may highlight the need for improving operational capabilities of TSPs, but more importantly for effectively integrating civil protection authorities into NEAMTWS and strengthening tsunami education programs.

Keywords: Mediterranean sea, Tsunami, Earthquake, Tsunami service providers, Tsunami early warning, Bodrum, Kos

Background

Turkey–Greece border in the Mediterranean Sea ruptured to a strong earthquake on July 20, 2017. According to the US Geological Survey (USGS), the epicenter was at 36.929°N and 27.414°E located 12 km to Kos in Greece and 13 km to Bodrum in Turkey (Fig. 1). This earthquake, registering a moment magnitude (Mw) of 6.6, occurred at the depth of 7 km with an origin time at 22:31:11 UTC according to the USGS. The seismological parameters of the event from the European-Mediterranean Seismological Center (EMSC) were as follows: epicenter, 36.96°N and 27.45°E; origin time, 22:31:11 UTC; moment magnitude, 6.6; and focal depth, 2 km. The duration of the earthquake was ~ 16 s (Saltogianni et al. 2017). Two deaths were reported following the earthquake along with around 500 injured. The earthquake received intense local/regional media attention as it occurred in a touristic place where many tourists, mainly from Europe, were spending their summer vacation. This earthquake was preceded by the M 3.1 foreshock, which occurred nearby the mainshock's epicenter at ~ 20 min before the mainshock, and by subsequent three $M \geq 1$ earthquakes.

*Correspondence: mohammad.heidarzadeh@brunel.ac.uk
[1] Department of Civil and Environmental Engineering, Brunel University London, Uxbridge UB8 3PH, UK
Full list of author information is available at the end of the article

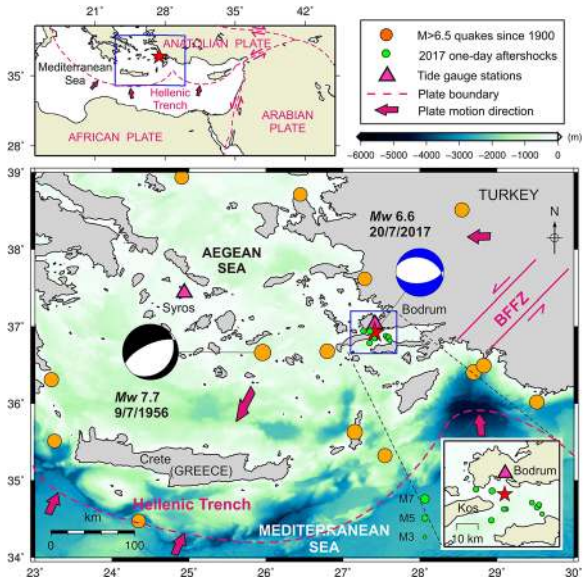

Fig. 1 Location map showing the epicenter (red star) and mechanism of the 20 July 2017 Bodrum–Kos earthquake. Locations of two tide gauges (Bodrum and Syros) are shown by pink triangles. Green circles show 1-day aftershocks ($M \geq 4$) from the USGS catalog. The mechanism for the 2017 event is taken from the USGS catalog. Orange circles are $M \geq 6.5$ earthquakes since 1900 AD obtained from the USGS catalog. The magnitude and mechanism of the 1956 event is obtained from USGS and Okal et al. (2009), respectively. Plate motion direction arrows and fault zones shown in this figure are based on those in Ozel et al. (2011) and Ebeling et al. (2012). *BFFZ* Burdur–Fethiye fault zone

Following the 20 July 2017 earthquake, two major seismic clusters (clusters A and B, Fig. 2a) were triggered and many aftershocks were generated in the source region (Fig. 2a). Approximately 1500 aftershocks with $M \geq 2.0$ were observed on August 11, 2017 (Fig. 2b). The triggered seismic cluster A was located approximately 30 km northeast of the mainshock which started on July 24, 2017 and included approximately 60$M \geq 2.0$ earthquakes (Fig. 2c). Cluster B was located at the northeastern edge of the source region which was typically activated on 7 August and followed by the largest aftershock (Mw 5.1) in this sequence (as of August 11, 2017). Possible mechanisms for the triggering of these seismic clusters are static stress changes imparted by the mainshock (e.g., Ishibe et al. 2015), the dynamic stress changes due to the passage of seismic waves (e.g., Hill et al. 1993), and/or decreases in failure strength due to increases in pore fluid pressure (e.g., Hubbert and Rubey 1959).

Based on the field surveys by Yalçiner et al. (2017), a moderate tsunami was generated following the earthquake reaching a maximum runup of 1.9 m along a dry stream at Gumbet bay (West of Bodrum, Turkey) and producing an average runup of ~ 0.6 m in the near-field around the city of Bodrum which flooded many nearshore restaurants and damaged boats mainly in the Gumbet bay (Yalçiner et al. 2017). A maximum runup of 1.5 m was observed in Kos Island (Yalçiner et al. 2017). No death was reported due to the tsunami. Details of the tsunami field survey are available in Yalçiner et al. (2017). Tsunami warnings were disseminated by the Tsunami Service Providers (TSPs) within the Intergovernmental Coordination Group, North East Atlantic, Mediterranean and Connected seas Tsunami Warning System (ICG/NEAMTWS). The EMSC disseminated a twitter message advising local people to avoid beaches, despite having no mandate for disseminating such a message and being out of their area of competence.

The epicentral region is an active seismic zone due to the presence of three main tectonic plate borders: African, Arabian, and Anatolian plates (Fig. 1). To the south of the epicenter, the Hellenic subduction zone is subducting beneath the Anatolian microplate; to the east, the Anatolian microplate is in strike-slip motions along its northeast and southeast boundaries with the Eurasian and Arabian plates, respectively. As shown in Fig. 1, the 2017 Mw 6.6 event occurred as an intraplate earthquake in the Aegean Sea region within the Anatolian microplate which is part of the Eurasian Plate. According to Kurt et al. (1999), the epicentral area is under a N–S extensional tectonic regime (35–40 mm/year according to Ebeling et al. 2012) which is most probably attributed to the westerly escape of the Anatolian plate in response to the collision of the African, Eurasian, and Arab plates. At least 14$M \geq 6.5$ earthquakes occurred in the region since 1900 AD based on the USGS catalog (https://earthquake.usgs.gov/earthquakes/search/). Among these large earthquakes, the largest one is the 9 July 1956 Amorgos event (M 7.7) (Fig. 1) which caused a death toll of 53 from both earthquake and tsunami, and the observed tsunami runup was up to 30 m (Ambraseys 1960; Okal et al. 2009). The most recent tsunami in the Mediterranean basin occurred on March 21, 2003 produced by an Mw 6.9 earthquake onshore Algeria, causing runup of ~ 2 m and moderate damage (Alasset et al. 2006; Sahal et al. 2009; Heidarzadeh and Satake 2013a).

The July 2017 Bodrum–Kos earthquake and tsunami is analyzed in this study to add insights into tsunami hazards in the Mediterranean basin by providing a source model and conducting waveform and spectral analyses as well as aftershock analysis. Although powerful tsunamis from $M > 8$ earthquakes occur almost annually in the Pacific Ocean (e.g., Synolakis et al. 2002; Fritz et al. 2012; Suppasri et al. 2013; Satake 2014; Heidarzadeh et al. 2016a; Shimozono and Sato 2016; Saito 2017; Ishibe et al. 2017), such events are less frequent in the Mediterranean Sea. Therefore, analysis of this moderate tsunami

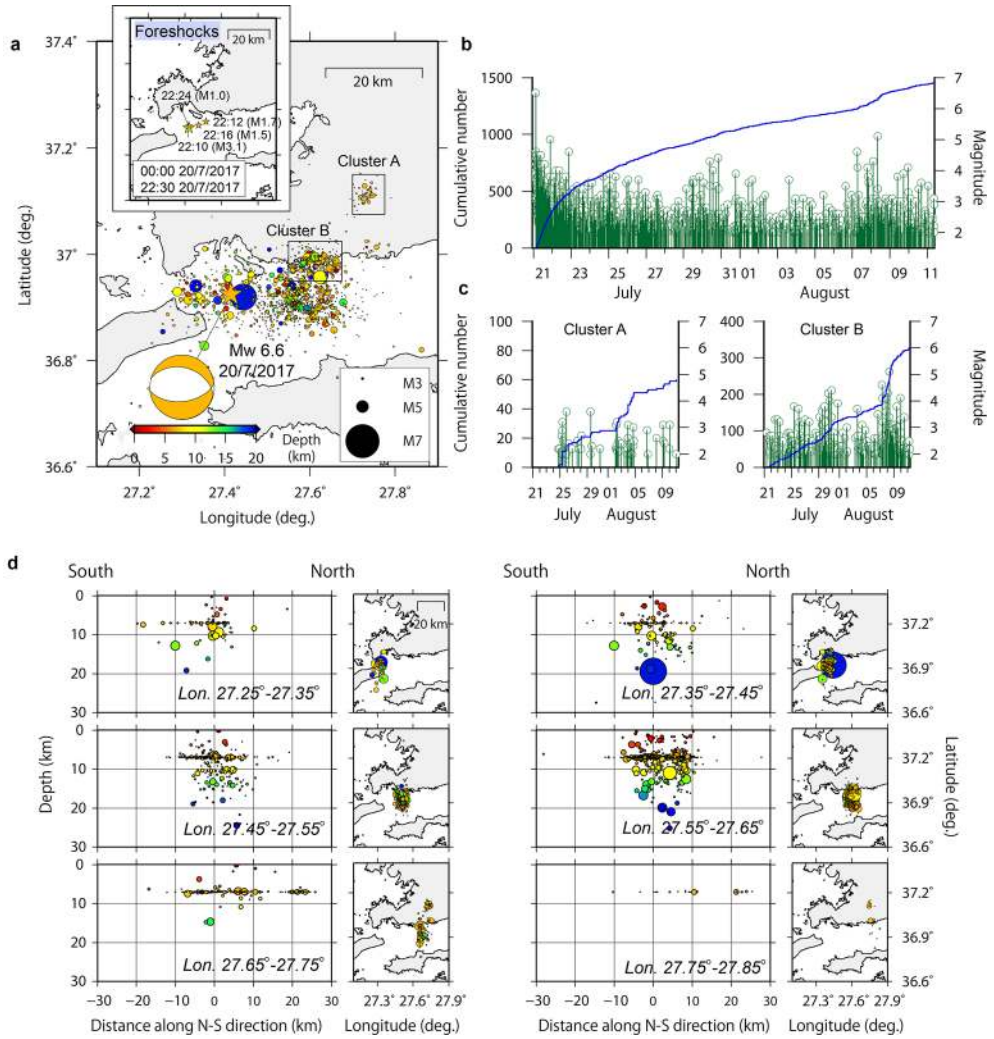

Fig. 2 Aftershock analysis for the 20 July 2017 Bodrum–Kos earthquake in Turkey. **a** Distribution of aftershocks ($M \geq 2.0$, depth ≤ 100 km) from the catalog provided by AFAD (Disaster and Emergency Management Authority, Earthquake Department, Turkey). The color map of the circles shows the hypocentral depth. The inset shows the hypocenter distribution of foreshocks on the day of the 2017 Bodrum–Kos earthquake. **b**, **c** Cumulative frequency curve (blue) and magnitude–time diagram (green) for the entire region and for two seismic clusters of A and B, respectively. **d** Cross sections of aftershock hypocenters at various longitude ranges (left panels) and their epicentral projections (right panels)

contributes toward tsunami assessment and awareness in this enclosed basin and tests the functional performance of TSPs in the NEAMTWS region. Here, we first report tide gauge records of the tsunami; second, conduct spectral analyses to reveal spectral content of the tsunami; and third, perform numerical modeling of tsunami and aftershock analysis to provide insights on the tsunami source. Aftershock analysis helps to identify the location of the fault plane (e.g., 1-day aftershocks). It is widely accepted to place the fault plane on the area around the epicenter where most of the aftershocks occurred (Satake et al. 2013). Spectral analysis helps to estimate the dimensions of the fault plane (length and width) using the tsunami phase velocity equation (Equation 5 in Heidarzadeh and Satake 2015b). Information from aftershock analysis and tsunami spectral analysis leads to effective tsunami simulations. We also discuss the response from the operational national and regional tsunami warning systems in the Mediterranean Basin to this tsunami.

Data and methods

Two tide gauge records of the tsunami were used in this study at Bodrum (Turkey) and Syros (Greece) located at distances of 13 and 230 km from the epicenter, respectively (see Fig. 1 for locations and Fig. 3 for the waveforms). The Bodrum and Syros records have

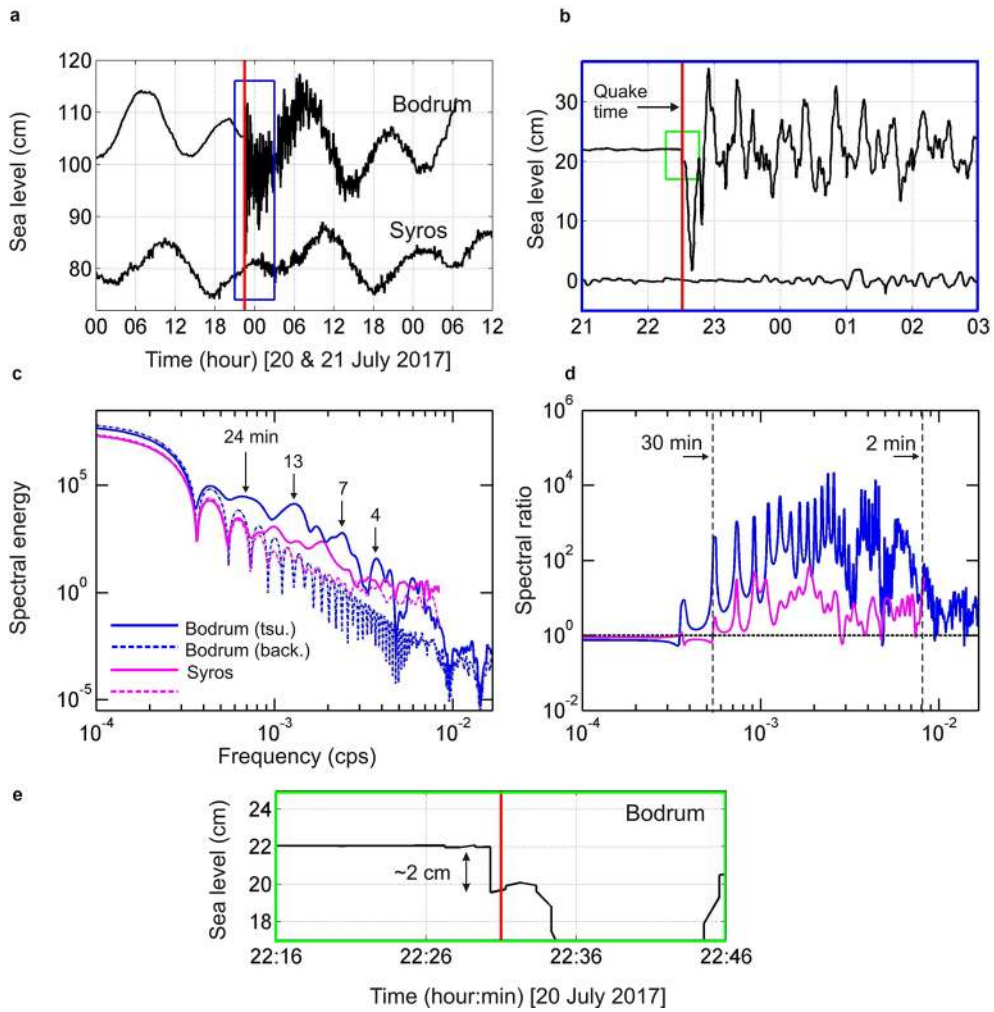

Fig. 3 Original records **a** and de-tided waveforms **b** of the 20 July 2017 Bodrum–Kos tsunami in Bodrum (Turkey) and Syros (Greece). **c**, **d** Spectra and spectral ratios at these two stations. *tsu* and *back* represent tsunami and background signals, respectively. **e** The enlarged view of the green rectangle shown in (**b**). In (**e**), the seafloor uplift of ~ 2 cm looks occurring 30 s before the earthquake time. Obviously, the uplift occurred simultaneously at the earthquake origin time (red vertical line); the 30 s shift can be attributed to the temporal resolution of the instrument

sampling intervals of 0.5 and 1 min, respectively. Tidal signals were removed from the original records by filtering the time-series applying the Butterworth Infinite Impulse Response digital filters in Matlab with the transfer coefficients of 5th-order and cutoff period of 90 min (Mathworks 2017). For Fourier analysis, which is a time-independent analysis, the Welch's (1967) averaged modified-periodogram technique was applied using time-series windows with length of 90 min and 50% of overlaps. We also applied the spectral ratio concept of Rabinovich (1997) to separate tsunami spectral content from non-tsunami sources by dividing the spectral powers of tsunami part of the waveforms to that of the background part (i.e., before tsunami arrival) (Vich and Monserrat 2009; Rabinovich et al. 2013; Heidarzadeh and Satake 2014, 2015a, b; and Heidarzadeh et al. 2016a). For spectral ratio analysis, we applied the original tsunami records rather than the filtered waveforms. The length of the background signal was the same as that of the tsunami signal at each station. Waveform segments of 8 and 3 h were used for the spectral ratio analyses at Bodrum and Syros stations, respectively.

The tsunami numerical package of Satake (1995) was used here for tsunami simulations on the GEBCO-2014 digital bathymetry with the resolution of 30 arc-seconds (Weatherall et al. 2015). Time step was 1.0 s for linear simulations. As inundation on dryland was not included in our simulations, such a bathymetry is adequate (e.g., Heidarzadeh et al. 2016a). According to Heidarzadeh et al. (2016b), linear and non-linear tsunami simulations

give similar results as long as the waves are prevented from inundation on dryland. Initial coseismic seafloor deformation was calculated using the Okada (1985) dislocation model. Fault parameters of strike, dip, and rake angles were based on the W-phase focal mechanism solution of the USGS. Other fault parameters (length, width) were calculated using empirical equations of Wells and Coppersmith (1994). Tsunami simulations were conducted for seafloor deformation from both nodal planes (NP) consisting of strike, dip, and rake angles of 285°, 39°, and − 73°, respectively, for NP-1 and respective values of 84°, 53°, and − 103° for NP-2. Length and width of the fault were fixed at 25 and 15 km and the slip value was determined by using a trial-and-error approach and by changing the slip value in the range of 0.3–0.8 m, with the increment of 0.1 m, in order to match the observed and simulated tsunami records in the near-field (i.e., Bodrum tide gauge). The quality of match between observation and simulations was judged based on visual looks at the simulated and observed waveforms. Top depth of the source fault was taken as 7 km because a hypocentral depth of 2–11 km was reported by various agencies (Table 1). The fault planes NP-1 and NP-2 included the epicenter. Locations of aftershocks guided the fault location. The fault plane was placed on the area around the epicenter where most of the aftershocks occurred. We acknowledge that the location of aftershocks can be associated with some errors because we did not relocate the aftershocks for this study. The source model that we calculate here has a focal mechanism based on the USGS's W-phase, is guided by the aftershock locations, and is confirmed with the tsunami tide gauge records.

Table 1 Earthquake fault parameters issued in the tsunami messages by various ICG/NEAMTWS TSPs operating in the eastern Mediterranean Basin for the 20 July 2017 Bodrum–Kos earthquake

	CAT-INGV	KOERI-RETMC	NOA/HL-NTWC	EMSC	USGS
Origin time (UTC)	22:31	22:31	22:31	22:31:11	22:31:11
Magnitude	Mw 6.8	Mw 6.6	ML 6.4[a]	Mw 6.6[b]	Mw 6.6
Depth (km)	10	11	10	2	7
Lat (°N)	36.90	36.96	36.95[c]	36.96	36.929[e]
Lon (°E)	27.46E	27.51	27.42[d]	27.45	27.414

For comparison, revised parameters from EMSC and USGS are also provided

[a] Local magnitude

[b] Initial value was 6.7

[c] Initial value was 36.96

[d] Initial value was 27.59

[e] Initial value was 36.925

Tsunami waveforms and physical properties

Figure 3 presents the original tsunami records (Fig. 3a) and de-tided waveforms (Fig. 3b). The de-tided waveforms reveal that the Bodrum tide gauge station was uplifted ~ 2 cm due to the earthquake and thus the tide gauge record at Bodrum shows an immediate decrease of ~ 2 cm (Fig. 3e). Such coseismic uplift of a tide gauge station also was observed during the 2016 Kaikoura (New Zealand) earthquake (Heidarzadeh and Satake 2017). Tsunami arrival is clear at the Bodrum station by initial depression wave, while it is not clear at the Syros station. The maximum trough-to-crest tsunami amplitudes are 34.1 and 3.3 cm at these two stations, respectively, indicating 20 times attenuation of tsunami amplitude for traveling 230 km from the epicenter to the Syros station. Far-field tsunami propagation is a function of water depth at the tide gauge location, source directivity, and wave reflection and refraction along the tsunami path (Heidarzadeh et al. 2015c, 2016a). Such strong attenuation of the tsunami amplitudes can be attributed to the numerous bathymetric features and islands existing in the region. Duration of tsunami oscillations is around 1 day at the Bodrum station (Fig. 3a).

Fourier analysis for both tsunami and background signals reveals multiple peak periods at 24, 13, 7, and 4 min (Fig. 3c). Tsunami signals show significant larger spectral energy levels at the aforesaid periods than the background signals at both stations. By producing spectral ratio plots (Fig. 3d), it is demonstrated that tsunami period band is 2–30 min. For comparison, tsunami wave periods can be up to around 60 min for large tsunamis such as the 2011 off-Tohoku (Japan) event (Heidarzadeh and Satake 2013b). It is worth noting that the value of spectral ratio is around one for the period > 30 min indicating a classic case for tsunami spectral ratio studies. The value of tsunami spectral ratio is normally one for non-tsunami period bands (i.e., period > 30 min and < 2 min). The multiple peaks and troughs existing in the background spectra and the spectral ratios are due to the stepwise nature of the background signals caused by rounding the tide gauge recordings to two decimal places; they do not affect the overall results though they affect the appearance of the plots. It can be inferred from Fig. 3d that the dominating tsunami period band is 7–13 min because the maximum spectral energy is seen within this period band at both stations. Dominating tsunami period band is referred to as the period band that contains the maximum spectral energy as shown in tsunami spectra and spectral ratio plots (Fig. 3c, d).

Source model

Tsunami simulations and comparison with observed waveforms are presented in Fig. 4 for both nodal planes NP-1 and NP-2 and for the slip value of 0.4 m. Slip value of 0.4 m was determined after several simulations using slip range of 0.3–0.8 m; this optimum slip value (i.e., 0.4 m) produced the best fit with the near-field tsunami observation at south of Bodrum peninsula both in terms of maximum depression and elevation waves. Best model means a source model that produces the closest match between tsunami observations and simulations both in terms of wave amplitudes and periods. Assuming a rigidity of 3×10^{11} dyne/cm^2 such a fault results in a seismic moment and a moment magnitude of 4.5×10^{25} dyne-cm and 6.3, respectively. Calculated seafloor deformation (Fig. 4a) confirms 1–2 cm of coseismic uplift at the Bodrum station for both NP-1 and NP-2. In general, both tsunami observations at Bodrum and Syros are fairly reproduced given the moderate size of the tsunami. At Bodrum, the tsunami period is reproduced well. Although the maximum simulated depression amplitude is slightly smaller than that of observation, and the maximum simulated elevation amplitude is slightly larger, the simulated trough-to-crest height is same as that of observation. Snapshots of tsunami propagation at different times (Fig. 5) reveal strong scattering and reflections of the waves due to the bathymetric features which contribute to rapid dissipation of wave energy and amplitudes. This is possibly the reason for strong tsunami amplitude attenuation in Syros at the distance of 230 km from the source.

The simulated waveforms from both NPs look similar which can be attributed to the small difference between

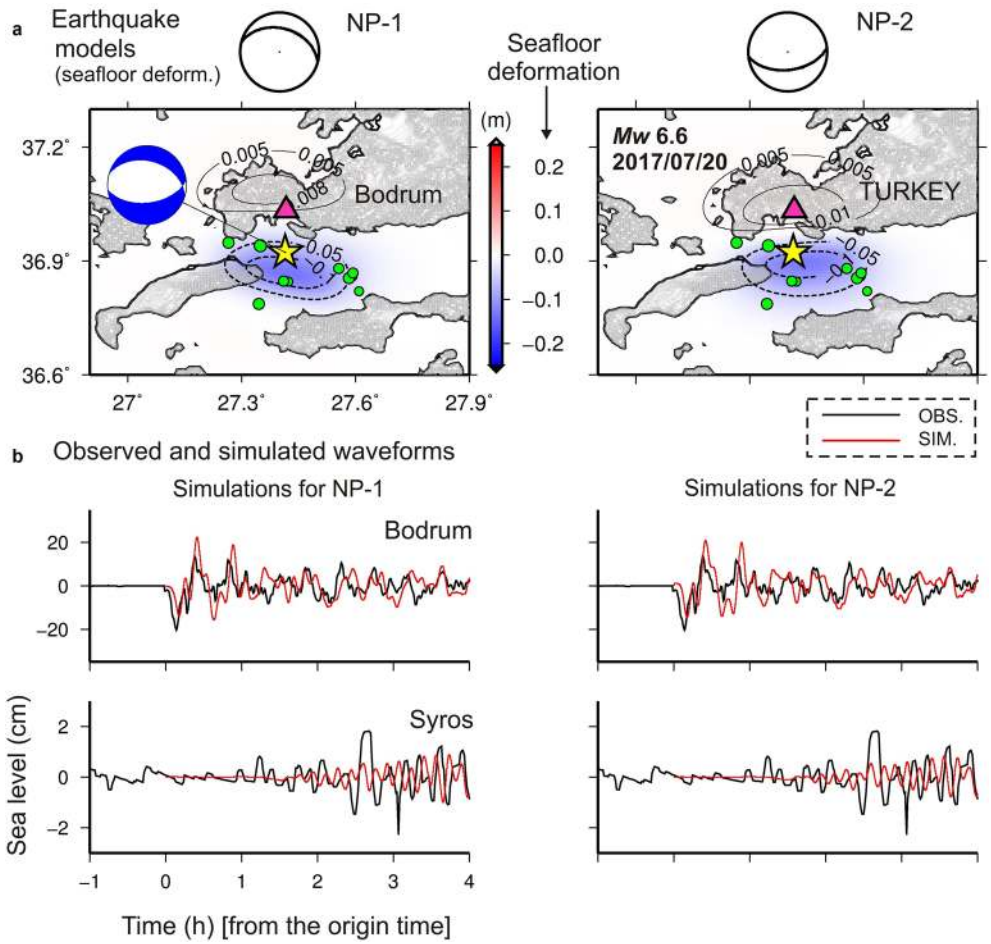

Fig. 4 **a** Seafloor deformation from source models based on nodal planes 1 (left) and 2 (right) for slip values of 0.4 m for the 20 July 2017 Bodrum–Kos tsunami. Green circles show 1-day aftershocks ($M \geq 4$) from the USGS catalog. **b** Comparison of observations (black) and simulations (red) for NP-1 (left) and NP-2 (right)

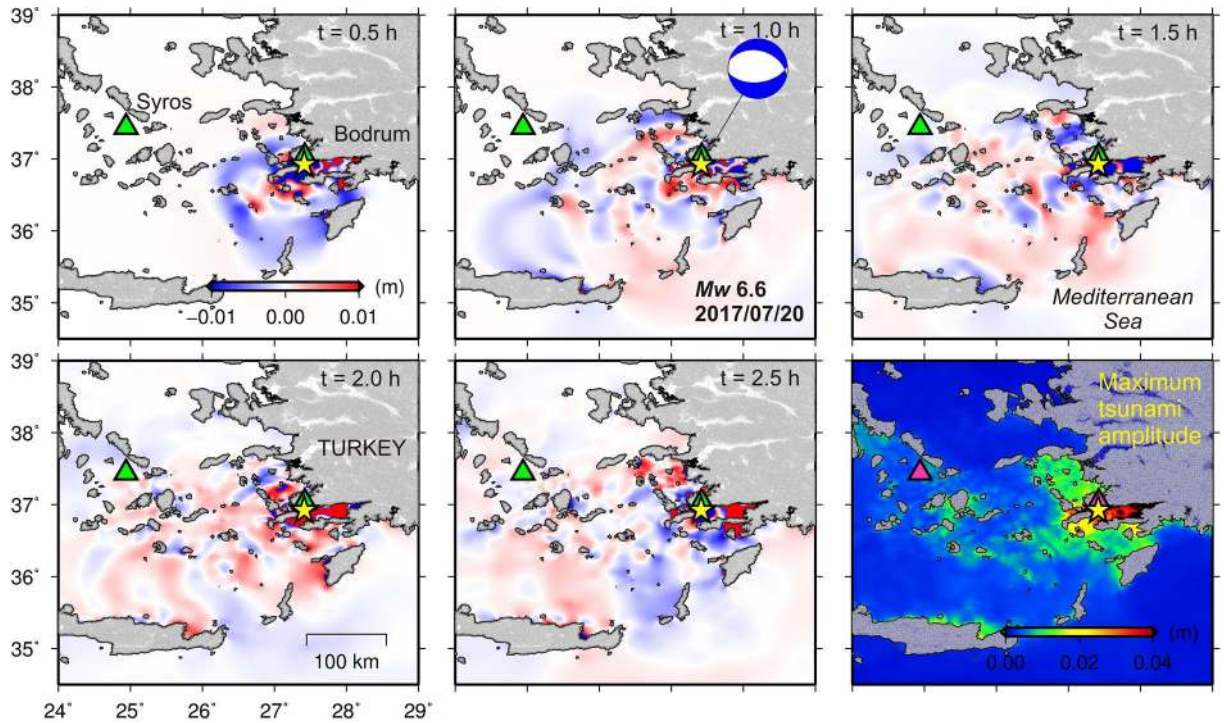

Fig. 5 Simulated snapshots at different times (the first five panels) and the maximum tsunami amplitude (the panel at bottom-right) for the 20 July 2017 Bodrum–Kos tsunami. These results are based on NP-1

coseismic seafloor deformation patterns obtained for the two NPs. Overall, tsunami simulations may indicate that a fault with length, width, and slip of 25 km, 15 km, and 0.4 m, respectively, was responsible for the July 2017 Bodrum–Kos tsunami. The current results are not capable of providing strong clues about which fault plane was the actual plane of the earthquake source (either northerly or southerly dipping). Seismological studies including our aftershock-hypocenter analysis (Fig. 2d) and the finite-fault model by Saltogianni et al. (2017) also have not been able to resolve the fault plane.

Response from tsunami warning systems and discussions

Since the establishment of the ICG/NEAMTWS more than 10 years ago, steady progress has been achieved towards the provision of tsunami watch services in the NEAM region (http://unesdoc.unesco.org/images/0024/002473/247393m.pdf). As of December 2017, France, Greece, Italy, and Turkey have National Tsunami Warning Centers (NTWC) and act as TSPs. Portugal is on the verge of similar capability. Spain has established its NTWC, and Israel is expected to follow in the near future. A Tsunami Information Centre for the NEAM region (NEAMTIC) has been set-up to provide tools and products to increase the awareness and the preparedness of the general public and to promote a better cooperation with the civil protection authorities (CPA). Regular communication tests and tsunami exercises, such as NEAMWAVE12 (http://unesdoc.unesco.org/images/0021/002189/218990e.pdf), NEAMWAVE14 (http://unesdoc.unesco.org/images/0023/002301/230172e.pdf), and the most recent NEAMWAVE17 (http://unesdoc.unesco.org/images/0025/002591/259196E.pdf) (November 2017) enabled the incorporation of the derived improvements into strategic planning for the future of NEAMTWS. Despite some limitations due to physical constraints, at the present time, a strong know-how and demonstrated capabilities of upstream components of tsunami warning system exist within the NEAMTWS.

During the 20 July 2017 tsunami event, all ICG/NEAMTWS tsunami service providers (TSPs), operating in the Eastern Mediterranean Basin, issued tsunami *Watch/Advisory*, *Ongoing*, and *End* messages to their subscribers and national CPAs. TSP messages are not designated to be publicly available. To receive them, official request should be made by designated authorities of ICG/NEAMTWS member states through the IOC Secretariat. It is the designated national authority's responsibility to implement relevant systems and adopt corresponding standard operational procedures to further communicate

the warnings to the public. TSPs that disseminated *Warning/Watch* messages during the 20 July 2017 event were CAT-INGV: Centro Allerta Tsunami Istituto Nazionale di Geofisica e Vulcanologia (Italy); KOERI-RETMC: Kandilli Observatory and Earthquake Research Institute-Regional Earthquake and Tsunami Monitoring Center (Turkey); and NOA/HL-NTWC: National Observatory of Athens-Hellenic National Tsunami Warning Centre (Greece). To define the alert levels, TSPs refer to the Decision Matrices (DM) embedded into their standard operational procedures. A DM is a set of empirical rules dealing with the possibility for tsunami generation based on the location of the epicenter, focal depth, and magnitude (Interim Operational Users Guide of NEAMTWS: http://ioc-unesco.org/index.php?option=com_oe&task=viewDocumentRecord&docID=8129; Ozel et al. 2011; Tinti et al. 2012; Papadopoulos 2015). While NOA/HL-NTWC utilizes the DM for the Mediterranean proposed by the ICG/NEAMTWS in 2010, CAT-INGV and KOERI-RETMC use a modified and less conservative DM in accordance with the recommendation of ICG/NEAMTWS in 2016 to determine the threat level information based on their best practices including scenario-based tsunami databases. During the 2017 Bodrum–Kos event, the earthquake parameters calculated and reported by these warning centers are provided in Table 1 and issue times of these messages are given in Table 2.

The waves from the 20 July 2017 Bodrum–Kos tsunami first receded around 5 min after the earthquake and then the first elevation wave arrived 12–13 min after the earthquake causing 60 m of inundation from the shoreline (Yalçıner et al. 2017). This is also confirmed by our numerical simulations (Fig. 4b). The earliest warning was a *Watch* message for local area (< 100 km distances) provided by CAT-INGV after 10 min from the origin time (Table 2), whose initial Mw estimation differed 0.2 units with respect to the final value. A *Watch* message indicates the potential for a tsunami where the expected wave height at the coastline and/or tsunami runup are greater than 0.5 and 1 m, respectively (Interim Operational Users Guide of NEAMTWS: http://ioc-unesco.org/index.php?option=com_oe&task=viewDocumentRecord&docID=8129). As for KOERI-RETMC and NOA/HL-NTWC, the first warning messages were considerably delayed (19 and 18 min after the origin time, respectively, Table 2). The alert levels of KOERI-RETMC and NOA/HL-NTWC were same as CAT-INGV. Based on the observed tsunami phenomena, we conclude that this alert level was appropriate. Nevertheless, even if the desirable time limit of ~ 10 min was achieved by KOERI-RETMC and NOA/HL-NTWC for the issuance of the initial warning messages, the other challenge would be the timely transfer of the message to the public at risk through the CPAs. It should be further noted that timely and reliable warning messages require stable moment magnitude calculations as well as quick expert assessment on the ground.

Table 2 Tsunami warning types and issue times of messages disseminated by ICG/NEAMTWS TSPs operating in the Eastern Mediterranean Basin for the 20 July 2017 Bodrum–Kos tsunami

Various TSPs within ICG/NEAMTWS	CAT-INGV	KOERI-RETMC	NOA/HL-NTWC
WATCH Message time (h: min, UTC)	22:41	22:50	22:49
Time interval after the origin time (min)	10	19	18
ONGOING message time (h: min, UTC)	01:02	23:32	01:53
END message time (h: min, UTC)	01:46	01:30	02:37

Earthquake origin time was July 20, 2017 at 22:31 UTC according to USGS

For most of the Eastern Mediterranean, tsunami hazard is a local (near-field) phenomenon and while the international and intergovernmental tsunami warning system (i.e., NEAMTWS) addresses the requirements for basin-wide tsunami threats, special focus is necessary for near-field tsunami threat due to its short arrival time (e.g., Synolakis and Kong 2006; Synolakis and Bernard 2006; Papadopoulos and Fokaefs 2013). The near-field tsunami threats are a challenge for tsunami warning systems around the world because of the short tsunami travel times (e.g., 15–20 min) and incapability of the current technologies to accurately estimate earthquake magnitudes in such a short time (e.g., Ozaki 2011). It is believed that the earthquake ground shaking is the first warning message for the coastal communities in the area emphasizing the importance of tsunami awareness and education for coastal communities (e.g., Synolakis and Okal 2005; Satake 2014). The components of tsunami warning systems in the near-field conditions of the Mediterranean Basin have been discussed by a number of authors among which are Ozel et al. (2011), Papadopoulos and Fokaefs (2013), and Necmioglu (2016).

The Bodrum–Kos tsunami showed that it is necessary to increase the number of tidal gauge stations and to establish offshore buoy measurement systems in the Mediterranean basin because very few tsunami measurement data are available for this event due to the sparse distribution of the sea level stations. Moreover, there have been recent improvements in tsunami warning system technologies which may help to directly use the tsunami measurements for efficient tsunami warnings in the near-field, e.g., tsunami assimilations (Gusman et al. 2016). The implementation of such systems would require strong collaboration between NEAMTWS TSPs

at international level and all end users and local stakeholders at national level. The recent 20 July 2017 Bodrum–Kos earthquake and tsunami has indicated one more time that, regardless of the structure and capabilities of tsunami warning systems, the effectiveness of any near-field tsunami early warning depends on the awareness, education, preparedness, and risk perception of the general public in the coastal communities. Therefore, we conclude that there is a need to focus on local tsunami early warning as part of the community programs supported by TSPs and other relevant stakeholders, such as municipalities and local disaster and CPAs. This highlights the need for further efforts to effectively integrate the downstream components of a tsunami warning system, such as sirens of other means for disseminating tsunami alerts to the population by the CPAs. The procedures for evacuation planning and the need for CPAs to demonstrate and maintain the capability to effectively respond to a rare (but possibly devastating) event by carrying out regular drills and exercises should be further promoted within national programs. In this context, individual nations participating in the framework of ICG/NEAMTWS should also investigate the feasibility of adopting education and preparedness programs such as the US National Weather Service *TsunamiReady* program (https://www.weather.gov/tsunamiready/) in NEAMTWS.

Conclusions

The 20 July 2017 Bodrum–Kos earthquake (Mw 6.6) and tsunami and the response from various Tsunami Service Providers in the NEAMTWS region were studied. The main findings and concluding remarks are:

1. The tsunami recorded a maximum trough-to-crest height of 34.1 and 3.3 cm at the two tide gauge stations of Bodrum (12 km from the epicenter) and Syros (230 km from the epicenter), respectively. The maximum runup was 1.9 m in Bodrum. Duration of tsunami oscillations was around 1 day at the Bodrum station. Tsunami period band was 2–30 min with peak periods at 7–13 min.
2. Tsunami simulations using a fault model having length and width of 25 and 15 km, respectively, slip of 0.4 m, and fault parameters from both nodal planes (NP-1: strike, 285°; dip, 39°; and rake, − 73° and respective values of 84°, 53°, and − 103° for NP-2) almost equally reproduced the tsunami observations. Tsunami simulation was unable to resolve the fault plane; our aftershock-hypocenter analysis also failed to do so.
3. Three ICG/NEAMTWS TSPs supplied tsunami warnings following this event at different times: CAT-INGV (Italy) at 10 min; KOERI-RETMC (Turkey) at 19 min; and NOA/HL-NTWC (Greece) at 18 min. Apart from CAT-INGV, the response from the other two TSPs came relatively late (compared to the desired time of ~ 10 min), given the complexities of real-time earthquake analysis for reliable determination of Mw. It is argued that even if the warning time of ~ 10 min was achieved, it might not be sufficient in addressing near-field tsunami hazards. Despite considerable accomplishments of NEAMTWS since its establishment more than a decade ago, the experience from this short arrival-time tsunami highlights the need for further integration of CPAs and promoting education and preparedness programs for the people at risk as the tsunami hazard for the Mediterranean region is a near-field hazard. In this regard, it would be advisable to identify these issues as strategic priorities for the development of NEAMTWS.

Abbreviations

AFAD: Disaster and Emergency Management Authority, Earthquake Department, Government of Turkey; DM: decision matrices; EMSC: European-Mediterranean Seismological Center; ICG/NEAMTWS: Intergovernmental Coordination Group for the Tsunami Early Warning and Mitigation System in the Northeastern Atlantic; CAT-INGV: Centro Allerta Tsunami Istituto Nazionale di Geofisica e Vulcanologia (Italy); KOERI-RETMC: Kandilli Observatory and Earthquake Research Institute- Regional Earthquake and Tsunami Monitoring Center (Turkey); NOA/HL-NTWC: National Observatory of Athens-Hellenic National Tsunami Warning Center (Greece); TSPs: Tsunami Service Providers.

Authors' contributions

MH prepared the initial draft, conducted tsunami simulations and spectral analysis, and produced relevant figures and texts. ON critically analyzed the response from various Tsunami Service Providers (TSPs), prepared the two tables, and wrote "Response from tsunami warning systems and discussions". TI performed aftershocks analysis, produced Fig. 2, and wrote the relevant texts. ACY provided critical insights for the tsunami source, peak tsunami coastal amplitudes, wave motions, and the performance of the TSPs. All authors read and approved the final manuscript.

Author details

[1] Department of Civil and Environmental Engineering, Brunel University London, Uxbridge UB8 3PH, UK. [2] Kandilli Observatory and Earthquake Research Institute, Bogazici University, Istanbul, Turkey. [3] Association for the Development of Earthquake Prediction, Tokyo, Japan. [4] Department of Civil Engineering, Ocean Engineering Research Center, Middle East Technical University, Ankara, Turkey.

Acknowledgements

The manuscript benefited from constructive comments by Prof. Kenji Satake (Editor-in-Chief) before submission for which we are sincerely grateful. MH thanks Dr. Gerassimos A. Papadopoulos (National Observatory of Athens, Greece) for fruitful discussions on this event during the 2017 International Tsunami Symposium in Bali, Indonesia. The authors would also like to thank all of the organizations mentioned in the "Availability of data and materials" section, which provided the data and information used in this study. The manuscript benefited from review comments made by three reviewers appointed by the journal (Dr. Stefano Lorito and two anonymous reviewers) for which we are sincerely grateful.

Competing interests

The authors declare that they have no competing interests.

Availability of data and materials
IOC sea level monitoring facility (http://www.ioc-sealevelmonitoring.org/) was used for the tide gauge records. Data providers are General Command of Mapping for Bodrum (Turkey) and Hellenic Navy Hydrographic Service for Syros (Greece) tide gauge stations. Aftershocks data are from the catalog provided by AFAD (Disaster and Emergency Management Authority, Earthquake Department, Government of Turkey) (https://www.afad.gov.tr/en/). We also used Generic Mapping Tools (Wessel and Smith 1998) for drawing figures (http://gmt.soest.hawaii.edu/).

Ethics approval and consent to participate
Not applicable.

Funding
MH is grateful to the Brunel University London for the funding provided through the Brunel Research Initiative and Enterprise Fund 2017/18 (BUL BRIEF).

Publisher's Note

Received: 7 September 2017 Accepted: 6 December 2017
Published online: 16 December 2017

References

Alasset PJ, Hébert H, Maouche S, Calbini V, Meghraoui M (2006) The tsunami induced by the 2003 Zemmouri earthquake (Mw = 6.9, Algeria): modelling and results. Geophys J Int 166:213–226
Ambraseys NN (1960) The seismic sea wave of July 9, 1956 in the Greek archipelago. J Geophys Res 65:1257–1265
Ebeling CW, Okal EA, Kalligeris N, Synolakis CE (2012) Modern seismological reassessment and tsunami simulation of historical Hellenic Arc earthquakes. Tectonophysics 530:225–239
Fritz HM, Phillips DA, Okayasu A, Shimozono T, Liu H, Mohammed F, Skanavis V, Synolakis CE, Takahashi T (2012) The 2011 Japan tsunami current velocity measurements from survivor videos at Kesennuma Bay using LiDAR. Geophys Res Lett. https://doi.org/10.1029/2011GL050686
Gusman AR, Sheehan AF, Satake K, Heidarzadeh M, Mulia IE, Maeda T (2016) Tsunami data assimilation of Cascadia seafloor pressure gauge records from the 2012 Haida Gwaii earthquake. Geophys Res Lett 43(9):4189–4196
Heidarzadeh M, Satake K (2013a) The 21 May 2003 tsunami in the western Mediterranean Sea: statistical and wavelet analyses. Pure Appl Geophys 170(9):1449–1462
Heidarzadeh M, Satake K (2013b) Waveform and spectral analyses of the 2011 Japan tsunami records on tide gauge and DART stations across the Pacific Ocean. Pure Appl Geophys 170(6):1275–1293
Heidarzadeh M, Satake K (2014) Excitation of basin-wide modes of the Pacific Ocean following the March 2011 Tohoku tsunami. Pure Appl Geophys 171(12):3405–3419
Heidarzadeh M, Satake K (2015a) Source properties of the 17 July 1998 Papua New Guinea tsunami based on tide gauge records. Geophys J Int 202(1):361–369
Heidarzadeh M, Satake K (2015b) New insights into the source of the Makran tsunami of 27 November 1945 from tsunami waveforms and coastal deformation data. Pure Appl Geophys 172(3–4):621–640
Heidarzadeh M, Satake K (2017) Possible dual earthquake-landslide source of the 13 November 2016 Kaikoura, New Zealand Tsunami. Pure Appl Geophys 174(10):3737–3749
Heidarzadeh M, Satake K, Murotani S, Gusman AR, Watada S (2015) Deep-water characteristics of the trans-Pacific tsunami from the 1 April 2014 Mw 8.2 Iquique, Chile earthquake. Pure Appl Geophys 172(3):719–730
Heidarzadeh M, Harada T, Satake K, Ishibe T, Gusman AR (2016a) Comparative study of two tsunamigenic earthquakes in the Solomon Islands: 2015 Mw 7.0 normal-fault and 2013 Santa Cruz Mw 8.0 megathrust earthquakes. Geophys Res Lett 43(9):4340–4349
Heidarzadeh M, Murotani S, Satake K, Ishibe T, Gusman AR (2016b) Source model of the 16 September 2015 Illapel, Chile Mw 8.4 earthquake based on teleseismic and tsunami data. Geophys Res Lett 43(2):643–650
Hill DP, Reasenberg PA, Michael A, Arabaz WJ, Beroza G, Brumbaugh D, Brune JN, Castro R, Davis S, dePolo D, Ellsworth WL, Gomberg J, Harmsen S, House L, Jackson SM, Johnston MJS, Jones L, Keller R, Malone S, Munguia L, Nava S, Pechmann JC, Sanford A, Simpson RW, Smith RB, Stark M, Stickney M, Vidal A, Walter S, Wong V, Zollweg J (1993) Seismicity remotely triggered by the magnitude 7.3 Landers, California, earthquake. Science 260:1617–1623
Hubbert MK, Rubey WW (1959) Role of fluid pressure in mechanics of overthrust faulting, 1. Mechanics of fluid-filled porous solids and its application to overthrust faulting. Geol Soc Am Bull 70:115–166
Ishibe T, Satake K, Sakai S, Shimazaki K, Tsuruoka H, Yokota Y, Nakagawa S, Hirata N (2015) Correlation between Coulomb stress imparted by the 2011 Tohoku-oki earthquake and seismicity rate change in Kanto, Japan. Geophys J Int 201:112–134
Ishibe T, Ogata Y, Tsuruoka H, Satake K (2017) Testing the Coulomb stress triggering hypothesis for three recent megathrust earthquakes. Geosci Lett 4:5
Kurt H, Demirbağ E, Kuşçu İ (1999) Investigation of the submarine active tectonism in the Gulf of Gökova, southwest Anatolia–southeast Aegean Sea, by multi-channel seismic reflection data. Tectonophysics 305(4):477–496
Mathworks (2017) MATLAB user manual. The Math Works Inc., MA, p 282
Necmioğlu Ö (2016) Design and challenges for a tsunami early warning system in the Marmara Sea. Earth Planets Space 68:13. https://doi.org/10.1186/s40623-016-0388-2
Okada Y (1985) Surface deformation due to shear and tensile faults in a half-space. Bul Seismol Soc Am 75:1135–1154
Okal EA, Synolakis CE, Uslu B, Kalligeris N, Voukouvalas E (2009) The 1956 earthquake and tsunami in Amorgos, Greece. Geophys J Int 178(3):1533–1554
Ozaki T (2011) Outline of the 2011 off the Pacific coast of Tohoku Earthquake (Mw 9.0). Earth Planets Space 63(7):57
Ozel NM, Necmioglu O, Yalciner AC, Kalafat D, Erdik M (2011) Tsunami hazard in the eastern Mediterranean and its connected seas: toward a tsunami warning center in Turkey. Soil Dyn Earthq Eng 31(4):598–610
Papadopoulos GA (2015) Tsunamis in the European-Mediterranean region: from historical record to risk mitigation. Elsevier, Amsterdam, p 290. ISBN 978-0-12-420224-5
Papadopoulos GA, Fokaefs A (2013) Near-field tsunami early warning and emergency planning in the Mediterranean Sea. Res Geophys 3:24–31
Rabinovich AB (1997) Spectral analysis of tsunami waves: separation of source and topography effects. J Geophys Res 102(C6):12663–12676
Rabinovich AB, Candella RN, Thomson RE (2013) The open ocean energy decay of three recent trans-Pacific tsunamis. Geophys Res Lett 40:3157–3162
Sahal A, Roger J, Allgeyer S, Lemaire B, Hébert H, Schindelé F, Lavigne F (2009) The tsunami triggered by the 21 May 2003 Boumerdes–Zemmouri (Algeria) earthquake: field investigations on the French Mediterranean coast and tsunami modelling. Nat Haz Earth Sys Sci 9(6):1823
Saito T (2017) Tsunami generation: validity and limitations of conventional theories. Geophys J Int 210(23):1888–1900
Saltogianni V, Taymaz T, Yolsal-Çevikbilen S, Eken T, Gianniou M, Öcalan T, Pytharouli S, Stiros S (2017) Fault-model of the 2017 Kos-Bodrum (east Aegean Sea) Mw 6.6 earthquake from inversion of seismological and GPS data—preliminary report. http://web.itu.edu.tr/~taymaz/docs/2017-SALTOGIANNI-TAYMAZ-ETAL-KOS-BODRUM-EARTHQUAKE-PRELIMINARY-REPORT.pdf. Accessed on 4 Dec 2017
Satake K (1995) Linear and nonlinear computations of the 1992 Nicaragua earthquake tsunami. Pure Appl Geophys 144:455–470
Satake K (2014) Advances in earthquake and tsunami sciences and disaster risk reduction since the 2004 Indian ocean tsunami. Geosc Lett 1(1):15
Satake K, Fujii Y, Harada T, Namegaya Y (2013) Time and space distribution of coseismic slip of the 2011 Tohoku earthquake as inferred from tsunami waveform data. Bull Seismol Soc Am 103(2B):1473–1492
Shimozono T, Sato S (2016) Coastal vulnerability analysis during tsunami-induced levee overflow and breaching by a high-resolution flood model. Coastal Eng 107:116–126
Suppasri A, Shuto N, Imamura F, Koshimura S, Mas E, Yalciner AC (2013) Lessons learned from the 2011 Great East Japan tsunami: performance of tsunami countermeasures, coastal buildings, and tsunami evacuation in Japan. Pure Appl Geophys 170(6–8):993–1018

Synolakis CE, Bernard EN (2006) Tsunami science before and beyond Boxing Day 2004. Phil Trans R Soc Lon A 364(1845):2231–2265
Synolakis CE, Kong L (2006) Runup measurements of the December 2004 Indian Ocean tsunami. Earthq Spectra 22(S3):67–91
Synolakis CE, Okal EA (2005) 1992–2002: Perspective on a decade of post-tsunami surveys. In: Satake K (ed) Tsunamis: case studies and recent developments, 23rd edn., pp 1–30
Synolakis CE, Bardet JP, Borrero JC, Davies HL, Okal EA, Silver EA, Sweet S, Tappin DR (2002) The slump origin of the 1998 Papua New Guinea tsunami. Proc R Soc Lon A 458(2020):763–789
Tinti S, Graziani L, Brizuela B, Maramai A, Gallazzi S (2012) Applicability of the decision matrix of North Eastern Atlantic, Mediterranean and connected seas Tsunami Warning System to the Italian tsunamis. Nat Hazards Earth Sys Sci 12:843–857
Vich MM, Monserrat S (2009) Source spectrum for the Algerian tsunami of 21 May 2003 estimated from coastal tide gauge data. Geophys Res Lett 36:L20610
Weatherall P, Marks KM, Jakobsson M, Schmitt T, Tani S, Arndt JE, Rovere M, Chayes D, Ferrini V, Wigley R (2015) A new digital bathymetric model of the world's oceans. Earth Space Sci 2:331–345. https://doi.org/10.1002/2015EA000107
Welch P (1967) The use of fast Fourier transform for the estimation of power spectra: a method based on time averaging over short, modified periodograms. IEEE Trans Audio Electroacoust 15:70–73
Wells DL, Coppersmith KJ (1994) New empirical relationships among magnitude, rupture length, rupture width, rupture area, and surface displacement. Bull Seismol Soc Am 84(4):974–1002
Wessel P, Smith WHF (1998) New, improved version of generic mapping tools released. EOS Trans AGU 79(47):579. https://doi.org/10.1029/98EO00426
Yalçıner AC, Annunziato A, Papadopoulos G, Dogan GG, Guler HG, Cakir TE, Sozdinler CO, Ulutas E, Arikawa T, Suzen L, Kanoglu U, Guler I, Probst P, Synolakis C (2017) The 20th July 2017 (22:31 UTC) Bodrum/Kos earthquake and tsunami; post tsunami field survey report. http://users.metu.edu.tr/yalciner/july-21-2017-tsunami-report/Report-Field-Survey-of-July-20-2017-Bodrum-Kos-Tsunami.pdf. Accessed on 4 Dec 2017